A systematic characterization of Cwc21, the yeast ortholog of the human spliceosomal protein SRm300

MAY KHANNA,[1,4] HARM VAN BAKEL,[1,4] XINYI TANG,[1] JOHN A. CALARCO,[1,2] TOMAS BABAK,[1,2] GRACE GUO,[1] ANDREW EMILI,[1,2] JACK F. GREENBLATT,[1,2] TIMOTHY R. HUGHES,[1,2] NEVAN J. KROGAN,[3] and BENJAMIN J. BLENCOWE[1,2]

[1]Banting and Best Department of Medical Research, Terrence Donnelly Centre for Cellular and Biomolecular Research, University of Toronto, Toronto, Ontario M5S 3E1, Canada
[2]Department of Molecular Genetics, University of Toronto, Toronto, Ontario M5S 1A8, Canada
[3]Department of Cellular and Molecular Pharmacology, California Institute for Quantitative Biomedical Research, University of California at San Francisco, San Francisco, California 94158, USA

ABSTRACT

Cwc21 (complexed with Cef1 protein 21) is a 135 amino acid yeast protein that shares homology with the N-terminal domain of human SRm300/SRRM2, a large serine/arginine-repeat protein shown previously to associate with the splicing coactivator and 3′-end processing stimulatory factor, SRm160. Proteomic analysis of spliceosomal complexes has suggested a role for Cwc21 and SRm300 at the core of the spliceosome. However, specific functions for these proteins have remained elusive. In this report, we employ quantitative genetic interaction mapping, mass spectrometry of tandem affinity-purified complexes, and microarray profiling to investigate genetic, physical, and functional interactions involving Cwc21. Combined data from these assays support multiple roles for Cwc21 in the formation and function of splicing complexes. Consistent with a role for Cwc21 at the core of the spliceosome, we observe strong genetic, physical, and functional interactions with Isy1, a protein previously implicated in the first catalytic step of splicing and splicing fidelity. Together, the results suggest multiple functions for Cwc21/SRm300 in the splicing process, including an important role in the activation of splicing in association with Isy1.

Keywords: Cwc21; SRm300; spliceosome; splicing; snRNP

INTRODUCTION

Splicing of precursor (pre-)mRNA entails the excision of intron sequences followed by ligation of exons and requires the assembly of a complex macromolecular machine, the spliceosome. Formation of active spliceosomes requires the association of four small nuclear ribonucleoprotein particles (U1, U2, U4/U6, and U5-snRNPs) and at least 100 non-snRNP proteins with the pre-mRNA prior to splicing catalysis (Matlin and Moore 2007; Staley and Woolford 2009; Wahl et al. 2009).

Prior to splicing, a complex biogenesis pathway leads to the assembly of snRNPs. This involves the addition of a methylated cap structure to the snRNAs, and, with the exception of U6 snRNA, the association of common (Sm) and specific protein components in the cytoplasm prior to snRNP import into the nucleus. Most studies support the existence of a stepwise spliceosome assembly pathway in the nucleus in which U1 snRNP associates early with the 5′ splice site to form an ATP-independent "E complex" (Matlin and Moore 2007; Staley and Woolford 2009; Wahl et al. 2009). This is followed by the ATP-dependent association of U2 snRNP with the branch site to form a pre-spliceosomal "A complex." U4/U6 and U5 next assemble as a tri-snRNP to form the spliceosomal "B complex." Subsequent ATP-dependent rearrangements within this complex involving multiple protein–protein and protein–RNA contacts lead to the release of U1 and U4 snRNPs and result in the generation of a catalytically active "C complex" (Matlin and Moore 2007; Staley and Woolford 2009; Wahl et al. 2009). This complex consists of U2, U5, and U6 snRNAs and a set of conserved proteins (see below). Following the second step of the splicing reaction, excised introns in the form of lariats are released along with U2,

[4]These authors contributed equally to this work.

Reprint requests to: Benjamin J. Blencowe, Banting and Best Department of Medical Research, Terrence Donnelly Centre for Cellular and Biomolecular Research, University of Toronto, University of Toronto, Room 1016, 160 College Street, Ontario M5S 3E1, Canada; e-mail: b.blencowe@utoronto.ca; fax: (416) 946-5545.

Article published online ahead of print. Article and publication date are at http://www.rnajournal.org/cgi/doi/10.1261/rna.1790509.

U5, and U6 snRNAs. The lariats are debranched and degraded, and the dissociated snRNPs are then recycled for another round of splicing (Matlin and Moore 2007; Staley and Woolford 2009; Wahl et al. 2009).

Budding yeast (*Saccharomyces cerevisiae*) *CWC21* (complexed with *CEF1* protein 21) was first documented as a gene (*YDR482C*) encoding a protein of unknown function that bears sequence similarity with the N-terminal 95 amino acids of the human SR-related nuclear matrix protein of 300 kDa (SRm300) (Blencowe et al. 2000). SRm300 was identified by mass spectrometry of purified complexes containing SRm160, a protein that functions as a coactivator of constitutive and exonic enhancer-dependent splicing and that has also been implicated in the coupling of splicing and mRNA 3′-end processing (Blencowe et al. 1998, 2000; Szymczyna et al. 2003). Cwc21 was subsequently identified as the ortholog of Cwf21, a component of the *Schizosaccharomyces pombe* Cdc5 complex (Ohi et al. 2002). The homolog of Cdc5 in *S. cerevisiae* is Cef1, and complexes associated with both proteins are highly enriched in known or putative splicing factors. Among these is Prp19, which forms the "NineTeen Complex" (NTC), a subcomplex of the spliceosome that is required to generate catalytically active first step spliceosomal C complexes in yeast and mammalian cells (Chen et al. 1998; Ohi and Gould 2002; Chan et al. 2003; Chan and Cheng 2005). Recent studies have revealed that SRm300 and additional human proteins that are orthologs of components of the yeast NTC complex form part of a salt-resistant core of active C complexes (Bessonov et al. 2008). These findings suggest an intimate and conservative role for Cwc21 and SRm300 in the splicing process. However, the gene encoding *S. cerevisiae* Cwc21 is non-essential, and efficient immunodepletion of SRm300 from HeLa cell splicing extracts does not significantly alter the splicing efficiency of two different model pre-mRNA substrates (Blencowe et al. 2000). Nevertheless, knockdown of the *Caenorhabditis elegans* ortholog of SRm300 causes an early larval arrest phenotype (Longman et al. 2001), suggesting that it has one or more critical in vivo functions in metazoan development.

In order to gain insight into the function of Cwc21, and by inference the possible function of SRm300, we have applied systematic screens to elucidate the networks of genetic, physical, and functional interactions involving this gene and its protein product. Synthetic genetic array (SGA) analysis employing a *cwc21* deletion strain (*cwc21-Δ*) was used to survey positive and negative genetic interactions, tandem affinity purification (TAP) of tagged Cwc21 was employed to identify protein partners, and genome-wide tiling microarrays were used to study the impact on the yeast transcriptome of deletion of *CWC21*, alone and in combination with the deletion of interacting factors. Our results suggest that Cwc21 provides more than one function in the splicing process. Moreover, the results reveal a strong genetic, physical, and functional association between Cwc21 and Isy1, a non-essential yeast factor that also belongs to the NTC and that has been implicated in the activation of step I spliceosomes and splicing fidelity (Villa and Guthrie 2005).

RESULTS AND DISCUSSION

Quantitative genetic analysis of Cwc21

We used SGA analysis (Tong et al. 2001) in a high-density E-MAP (Epistatic Miniarray Profile) format (Schuldiner et al. 2005) to assess the genetic relationships between *cwc21* and ~500 genes with known or putative links to RNA processing (Wilmes et al. 2008). In this analysis, a viable strain deleted for *CWC21* was crossed with ~500 other viable yeast strains, each harboring a gene deletion for one of the other RNA processing-related factors. Automated scoring of colony sizes from the double mutant progeny afforded an indirect assessment of functional relatedness, since simultaneous deletion of pairs of genes operating in common processes and pathways more often results in altered cell growth than observed for deletion of pairs of genes that are not functionally related (Tong et al. 2001). Since this analysis is quantitative, both positive (e.g., suppression) and negative (e.g., synthetic lethality) genetic interactions can be detected.

Strong negative genetic interactions were detected in double mutant strains deleted for *CWC21* and genes encoding multiple factors involved in various stages of pre-mRNA splicing and the processes of sn(o)RNP biogenesis/turnover, RNA retention, and mRNA export (Fig. 1A). These factors include the U1 snRNP protein Mud2 (Abovich et al. 1994; Rutz and Seraphin 1999), the U2 snRNP/retention complex proteins Bud13 (Vincent et al. 2003; Dziembowski et al. 2004; Trowitzsch et al. 2008) and Ist3/Snu17 (Gottschalk et al. 2001; Trowitzsch et al. 2008), the U2 snRNP protein Lea1 (Caspary and Seraphin 1998), the U4/U6·U5 protein Snu66 (Stevens et al. 2001), the sn(o)RNA-associated Lsm7 protein (Tharun et al. 2000; Pannone et al. 2001; Fernandez et al. 2004), Ecm2 involved in U2/U6 helix formation (Xu and Friesen 2001), the cap-binding proteins Cbc2 and Sto1 (Das et al. 2006), snRNA/snRNP biogenesis protein Brr1 (Noble and Guthrie 1996a,b), the Cef1/NTC complex proteins Isy1 (Dix et al. 1999) and Cwc15 (Ohi et al. 2002), the splicing and mRNA export factor Npl3 (Flach et al. 1994; Lee et al. 1996; Kress et al. 2008), and a previously uncharacterized protein, Ynr004w (Fig. 1A; Volckaert et al. 2003). Where tested, these genetic interactions were confirmed using tetrad analysis (data not shown). Moreover, a subset of the genetic interactions has been independently observed in the accompanying study by Grainger et al. (2009).

Each gene in the E-MAP possesses a genetic interaction profile, which describes its interactions with all other genes in the map. This E-MAP profile thus provides a high-resolution

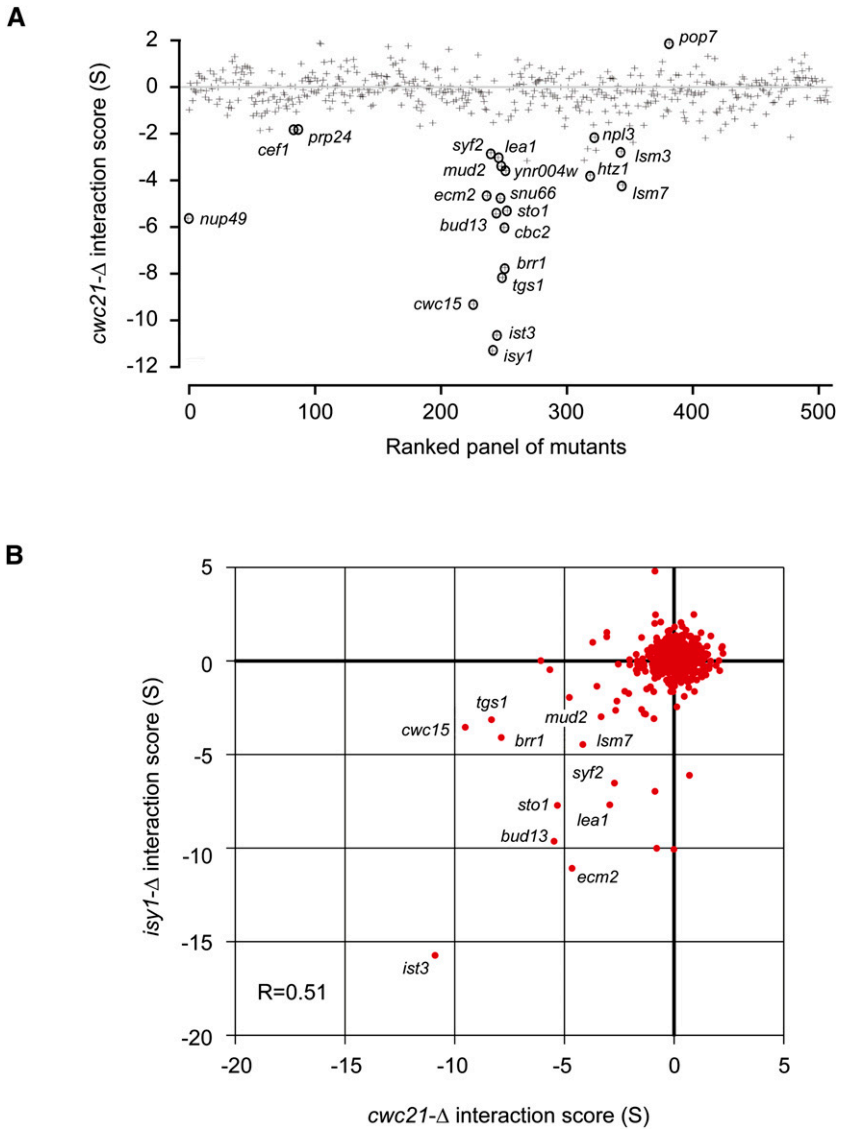

FIGURE 1. *CWC21* interacts genetically with genes encoding splicing factors. (*A*) Using SGA technology in a high-density E-MAP (epistatic miniarray profile) format, a strain harboring a deletion of *CWC21(cwc21-Δ)* was crossed to a panel of >500 mutants involved in various aspects of RNA processing (Wilmes et al. 2008). Growth rates of the double mutants were assessed by automated image analysis of colony size and interaction scores were derived as previously described (Schuldiner et al. 2005; Collins et al. 2006). Positive (e.g., suppression) and negative (e.g., synthetic lethality) genetic interactions are displayed above and below the zero baseline, respectively. (*B*) Scatterplot of genetic interactions observed for *cwc21* (*x*-axis) and *isy1* (*y*-axis) obtained from the RNA processing E-MAP.

genetic phenotype, and functionally related genes often have similar genetic phenotypic profiles (Schuldiner et al. 2005; Collins et al. 2007; Wilmes et al. 2008). When the genetic interaction data generated from the *cwc21-Δ* strain were compared to all other genetic profiles from the RNA processing E-MAP, the most highly correlated profile was that obtained from a deletion of *ISY1* (Fig. 1B). Interestingly, the strongest negative genetic interaction observed with *cwc21* was also with *isy1* (Fig. 1A). Taken together, these genetic data strongly suggest a functional role for Cwc21 in pre-mRNA splicing, and more specifically provide evidence for a functional interaction between Cwc21 and Isy1, the protein product of which functions in the first catalytic step of splicing and in splicing fidelity (see below). Moreover, multiple genetic interactions were observed with components of the U2 snRNP, including Lea1, Mud2, and Snu17, further suggesting that Cwc21 may function by associating with this snRNP particle. This proposal was supported by the experiments described below, which reveal that among the four spliceosomal snRNPs, Cwc21 predominantly interacts with U2 snRNP components.

A proteomic analysis of Cwc21-containing complexes

To further characterize the function of Cwc21, we purified its protein product along with associated components using the tandem affinity purification (TAP) procedure (Puig et al. 2001). The purified complexes were analyzed for both their protein and RNA composition, using ion trap mass spectrometry and a custom microarray (Hiley et al. 2005) designed to detect all major yeast noncoding RNAs.

Consistent with previous data from analyzing Cef1/Cdc5/NTC complexes and the genetic interaction data described above, our mass spectrometry analysis revealed that Cwc21 physically interacts with multiple spliceosomal components, including those found in Cef1/NTC complexes (Table 1; Ohi and Gould 2002). Moreover, also consistent with our genetic interaction data, the mass spectrometry results support possible additional splicing-related roles for Cwc21 including snRNP biogenesis, spliceosome disassembly, and mRNA export (see Table 1). Proteins detected by mass spectrometry as having high confidence interactions with Cwc21, some of which are also represented by the genetic interactions described above, include many spliceosomal proteins (Table 1, Isy1, Cef1, Cwc2, Cwc16, Spp2, Prp8, Prp45, Prp46, Syf2, Cdc40, Prp6, Snt309) and factors associated with snRNPs (Table 1, Lea1, Prp21, Bud31, Smd1, Smd3, Smb1, Smx3, Lsm5, Lsm6, Lsm8) and mRNA export (Table 1, Npl3). Additional Cwc21-interacting

TABLE 1. Proteins detected by mass spectrometry of TAP-tagged affinity-purified Cwc21 complexes

Protein	Description	Number of peptides	
		TAP-Cwc21 complex	TAP-Prp8 complex
Spliceosomal proteins			
Cwc21	Complexed with Cef1p; part of NTC	23	3
Npl3*	Yeast shuttling SR-like protein; promotes co-transcriptional splicing and mRNA export	5	3
Spp2	Promotes the first step of splicing	5	1
Cef1*	Associated with Prp19p and the spliceosome	4	3
Prp45	Required for splicing; ortholog of coactivator SKIP	4	2
Prp8	U4/U6-U5 component; lies at the catalytic center	3	62
Cwc16/Yju2	Following Prp2 promotes first catalytic splicing reaction; part of NTC	3	—
Cwc2	RNA splicing; part of NTC	2	—
Isy1*	Helps regulate fidelity of splicing with Prp16p; part of NTC	2	—
Prp46	Protein required for splicing in vivo; part of NTC	2	1
Syf2*	Involved in splicing and cell cycle progression	2	2
Cdc40	Important for catalytic step II of splicing and cell cycle progression	1	—
Ntr2	Spliceosome disassembly (forms a trimer with Ntr1 and Prp43)	1	—
Prp6	U4/U6-U5 component; splicing factor	1	10
Snt309	RNA splicing; part of NTC	1	1
snRNP proteins			
Lea1*	U2 snRNP component; putative homolog of human U2A snRNP	3	2
Prp21	Subunit of the SF3a splicing factor complex	2	2
Smd2	Core Sm protein; involved in snRNP biogenesis	7	13
Smd3	Core Sm protein; involved in snRNP biogenesis	5	18
Smb1	Core Sm protein; hypermethylate snRNA cap structure with Tgs1	2	9
Smd1	Core Sm protein; involved in snRNP biogenesis	2	14
Smx2	Core Sm protein; involved in snRNP biogenesis	2	—
Smx3	Core Sm protein; involved in snRNP biogenesis	1	3
Lsm5	Lsm (Like Sm) protein; part of heteroheptameric complexes	3	4
Lsm6	Lsm (Like Sm) protein; part of heteroheptameric complexes	2	4
Lsm8	Heteroheptameric complex also involved in nuclear RNA degradation	2	7
Bud31/Cwc14	Component SF3b subcomplex of U2 snRNP	1	—
Helicases			
Ded1	RNA helicase required for translation initiation	2	4
Brr2	RNA helicase required for disruption of U4/U6 base-pairing	1	9

Proteins also detected in a parallel affinity purification of Prp8p complexes are shown for comparison. An asterisk indicates a protein detected as having a genetic interaction with *cwc21* in the SGA screen (Fig. 1). All peptides for listed proteins were detected at a confidence of at least 99.6%.

proteins previously associated with splicing include two helicases (Table 1, Ded1, Brr2). The reciprocal interactions observed between Cwc21 and Prp8 are in agreement with results in the accompanying study that these proteins interact directly (Grainger et al. 2009).

It is worth noting that previous attempts to purify Cwc21 complexes using the TAP procedure did not yield stable or reproducible associations with splicing or other factors because these complexes are either in low abundance or unstable (Gavin et al. 2006; Krogan et al. 2006). In the present study, we found it necessary to scale up purifications several-fold to facilitate the reproducible detection of interacting factors. When we merged the mass spectrometry data obtained in the present study with data from a previous analysis of tagged yeast protein complexes purified by the TAP procedure (Collins et al. 2007), and clustered the combined data, we found that from the purification data, from >2000 proteins, Cwc21 clusters most closely with components of the Prp19 complex (Fig. 2A). These physical data, combined with the genetic interaction data, strongly suggest that Cwc21 is a functional component of the Cef1 complexes but that it also interacts with factors involved in linked steps of pre-mRNA processing, including snRNP biogenesis, spliceosomal disassembly, and mRNA export.

Cwc21 preferentially associates with snRNAs found in step I spliceosomes

Using a custom microarray containing tiled probes specific for most *S. cerevisiae* ncRNAs (Hiley et al. 2005), we next analyzed the RNA composition of Cwc21 complexes. RNA

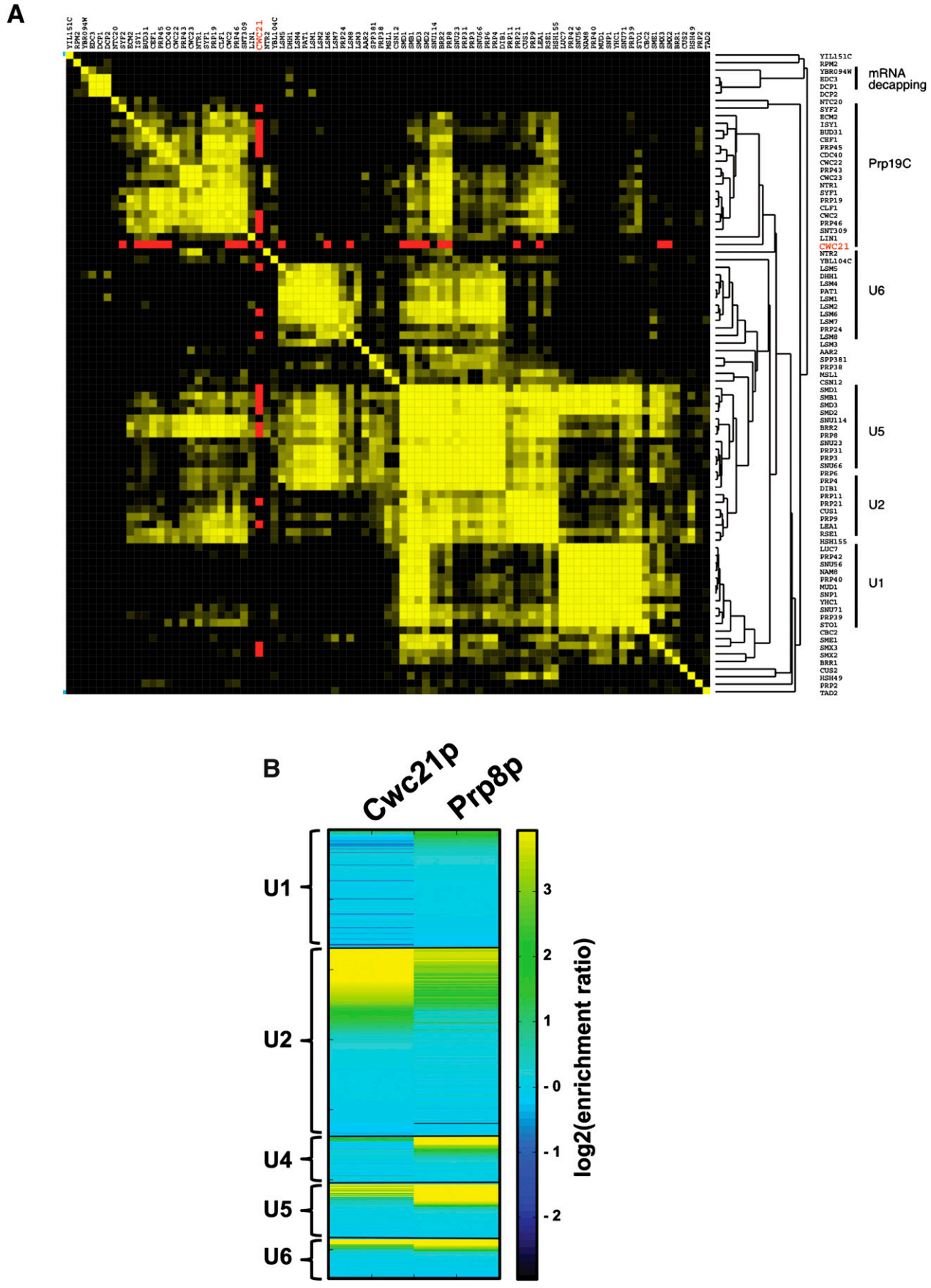

FIGURE 2. (Legend on next page)

was recovered from the TAP Cwc21 complexes used above for mass spectrometry analysis and directly labeled with fluorescent dyes and hybridized to the microarray, together with directly labeled total RNA (Leeds et al. 2006; Zhao et al. 2008). RNA recovered from the TAP-Prp8 complexes was analyzed in parallel for comparison and specificity-control purposes.

When sorting ncRNA probe signals on the basis of their relative enrichment in the TAP complexes compared to the total RNA channel, the strongest overall signals (as reflected by multiple independent probes specific for the same ncRNA) were observed for a specific subset of spliceosomal snRNAs (Fig. 2B). For each detected snRNA, probes displaying strongest to weakest signals from hybridization to snRNAs in the Cwc21 complexes were ordered from top to bottom in the plots shown in Figure 2B. The same probe ordering is shown in the adjacent plot for snRNAs detected in the purified Prp8 complexes, affording a direct comparison of the relative enrichment of snRNAs in the two complexes. In each case, only a subset of the probes specific for an enriched snRNA produced robust signals. This is not due to enrichment of snRNA fragments since the probes producing strong signals are specific for sequences that are distributed across the majority of the length of each snRNA, and intact snRNAs were detected in the recovered complexes by Northern blotting (data not shown). Instead, it is likely that stable secondary structures in the snRNAs prevent many of the microarray probes from hybridizing efficiently.

Consistent with the genetic interaction and mass spectrometry data described above indicating that Cwc21 is closely associated with U2 snRNP components (Figs. 1, 2A; Table 1), Cwc21 is predominantly associated with U2 snRNA. However, it is also specifically associated with U5 and U6 snRNAs. Little to no enrichment was detected for U1 and U4 snRNAs in the Cwc21 complexes. This pattern of snRNA association appears to be specific since the TAP Prp8 complexes are most strongly associated with U5, followed by U4 and U6 snRNAs, a result that is consistent with the previously reported stable and specific associations of this protein with free U5 snRNP and with the U4/U6•U5 tri-snRNP (Grainger and Beggs 2005). Together with the genetic and mass-spectrometry data demonstrating multiple interactions with Cef1/NTC factors, these results further suggest a role for Cwc21 at the core of spliceosomal complexes.

Functional interaction between Cwc21 and the splicing fidelity factor Isy1

Active spliceosomes are composed of both essential and non-essential proteins. An emerging role for certain non-essential spliceosomal proteins is in splicing fidelity. Among the best characterized of such proteins is Isy1 (Villa and Guthrie 2005). Through a series of elegant genetic and biochemical experiments, Guthrie and colleagues have shown that Isy1 is required for efficient splicing and that its deletion suppresses a cold-sensitive defect in an allele (*prp16-302*) of the gene encoding Prp16, a DEAH-box ATPase that transiently associates with the spliceosome to promote structural rearrangements required for the second chemical step of splicing. When *prp16-302* strains are grown at low temperatures, release of Prp16 from transitioning spliceosomes is stalled, and these complexes produce aberrant branchpoints at increased frequency. Deletion of *isy1* improves the growth of *prp16-302* strains, apparently by alleviating stalling and aberrant branch site selection. However, in the absence of Isy1 and the presence of wild-type Prp16, an increased rate of aberrant 3′ splice site selection is observed. These results suggested that Isy1 functions to promote the formation of active step I spliceosomes, whereas deletion of *isy1* favors premature release of Prp16, thereby promoting second-step chemistry, but at the expense of reduced fidelity in 3′ splice site recognition. The genetic and physical interactions detected between Cwc21 and Isy1 in the present study suggest that these two non-essential factors may act together during step I of splicing.

In order to investigate functional interactions between Cwc21 and Isy1, we used Affymetrix whole genome tiling microarrays to examine pre-mRNA splicing defects in RNA isolated from strains singly and doubly deleted for these genes. In the plots described below, data for all intron-containing genes were merged, and the ratios of probe signals in the mutant relative to wild-type strains were plotted, after normalizing to either exon signal so as to more clearly reveal relative effects on intron signals (Fig. 3A,B), or to all probes on the microarrays so as to also reveal relative effects on transcript levels (Supplemental Fig. 1).

Consistent with the absence of observable growth defects in *cwc21-Δ* strains, intron-containing genes did not display any pronounced defects in pre-mRNA processing (Fig. 3A). However, overall transcript levels were somewhat reduced for transcripts from intron-containing genes relative to

FIGURE 2. Association of Cwc21 with Prp19 (NTC) components and spliceosomal snRNAs. (*A*) The mass-spectrometry data shown in Table 1 were merged with data from two large-scale proteomics studies of tag-affinity-purified *S. cerevisiae* protein complexes (Gavin et al. 2006; Krogan et al. 2006; Collins et al. 2007) and hierarchical clustering of the merged data sets was performed. Of >2000 proteins, Cwc21 clusters most closely with components of the NTC complex. The clustergram shown represents a small portion of the entire set of clustered data (data not shown). (*B*) Microarray profiling of RNA recovered from tag affinity-purified Cwc21 and Prp8 complexes. RNA recovered following each affinity purification was directly labeled with Cy3 and Cy5 dyes and hybridized to a custom tiling microarray (Hiley et al. 2005) that detects non-coding RNAs. Signals were sorted from highest to lowest signal for each snRNA. The scale indicates $\log_2$ of the ratio of probe intensity in the pull-down to total RNA.

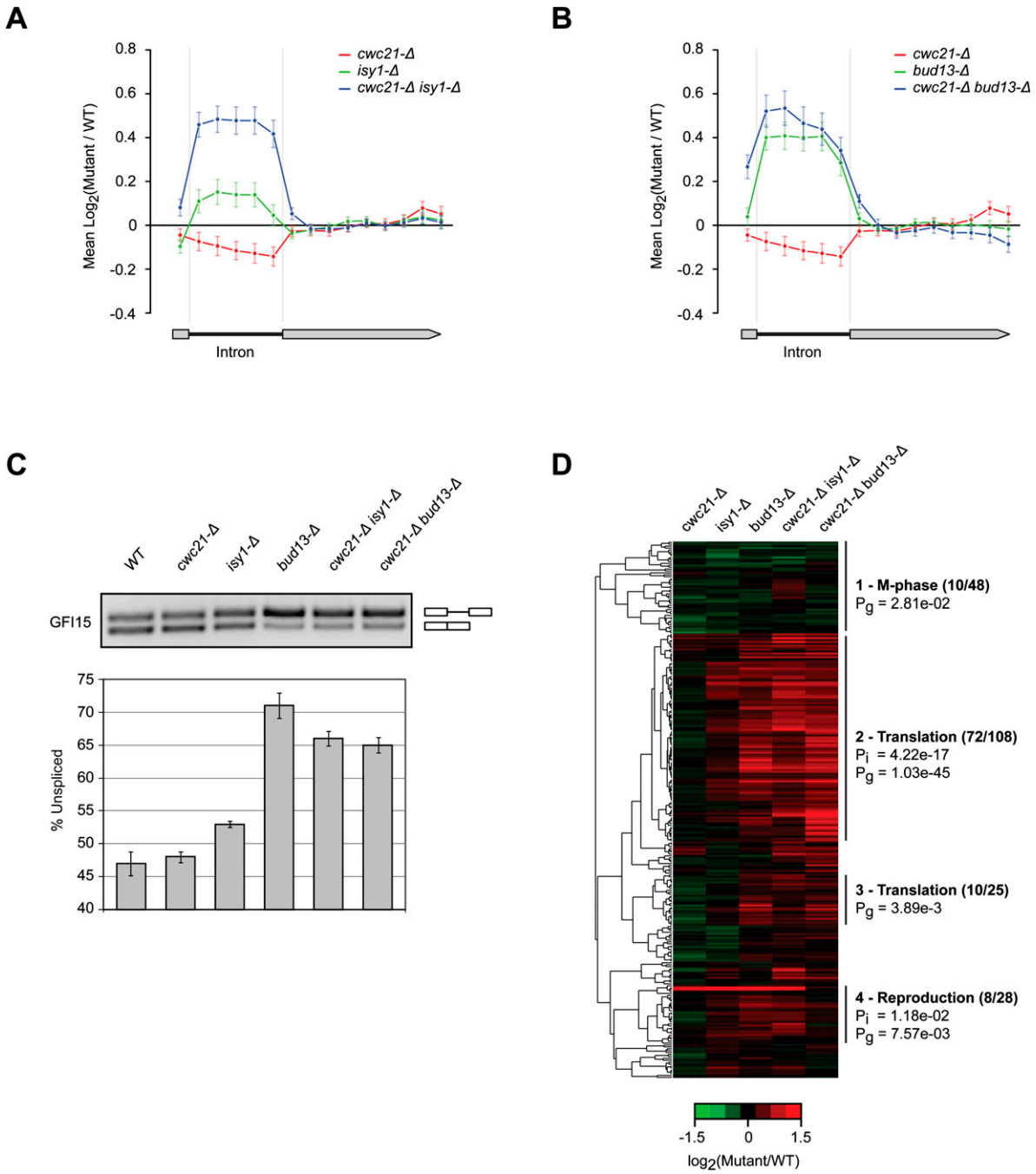

FIGURE 3. Widespread defects in pre-mRNA splicing in double mutant yeast strains lacking Cwc21. cDNA prepared from RNA purified from wild-type (WT) and single and double gene deletion (mutant) strains was labeled with Cy3 and Cy5 dyes and hybridized to *S. cerevisiae* genome-wide Affymetrix tiling microarrays. Normalized probe intensity signals were determined for all intron-containing transcripts, excluding tRNAs and dubious ORFs. After normalization of expression levels between the intron-containing genes using averages of all probe signals for exon sequences, the average $\log_2$ ratios of the mutant over wild-type expression differences were plotted in a fixed number of bins. (*A*) Plots of the average $\log_2$ ratios relative to WT for all intron-containing genes in the *cwc21-Δ* and *isy1-Δ* single and double mutant stains. (*B*) Plots of the average $\log_2$ ratios relative to WT for all intron-containing genes in the *cwc21-Δ* and *bud13-Δ* single and double mutant strains. Error bars in both plots indicate 95% confidence intervals. (*C*) Representative RT-PCR assay of spliced and unspliced transcripts from the GFI15 gene in the mutant strains analyzed by tiling microarrays. (*D*) Hierarchical clustering of the average expression level differences in intron sequences between mutants and WT strains, corrected for the mean signal across exons. Clusters are annotated for significantly enriched GO terms, with *P*-values calculated relative to a background set containing all genes (Pg) or intron- containing genes only (Pi). Additional clustering data and a list of genes in each cluster are provided in Supplemental Table 1.

transcripts from intronless genes in this deletion strain (Supplemental Fig. 1). Moreover, intron-containing transcripts relative to exon-containing transcripts from the same genes displayed a further reduction in signal in the *cwc21-Δ* strain (Supplemental Fig. 1). These effects could be due to a possible effect of *CWC21* deletion on transcriptional activity, in addition to modest effects on splicing leading to an accumulation of intron-containing transcripts that are subsequently degraded, possibly in part because of loss of nuclear retention and turnover of these transcripts by nonsense-mediated mRNA decay (NMD) (see below) (He et al. 1993; Sayani et al. 2008). In contrast, transcripts in the *isy1-Δ* strain displayed marked increases in intron signals relative to exon signals (Fig. 3A), and no overall reduction in transcript levels (Supplemental Fig. 1A). This observation is entirely consistent with the aforementioned findings that Isy1 is important for the efficiency of the first chemical step of splicing (Villa and Guthrie 2005).

Remarkably, in the double *cwc21-Δ isy1-Δ* mutant, splicing of transcripts from intron-containing genes was further disrupted, as observed from the overall significant increase in intron versus exon signals in this double mutant strain relative to either of the single deletion strains (Fig. 3A). Similar results have been observed in the accompanying study by Grainger et al. (2009). Interestingly, in the double *cwc21-Δ isy1-Δ* mutant, the reduced transcript levels seen in the *cwc21-Δ* mutant are suppressed (Supplemental Fig. 1B). A possible explanation for this is that pre-mRNAs in these strains are "trapped" in arrested spliceosomal complexes and therefore no longer subject to the same degree of turnover as in the *cwc21-Δ* mutant.

To assess whether the effects observed in the *cwc21-Δ* mutant reflect a more general requirement for Cwc21 in splicing in conjunction with its interacting factors, we next performed a tiling microarray analysis of RNA from strains singly and doubly deleted for *CWC21* and *BUD13*. As mentioned above, Bud13 is a component of the U2 snRNP, and it functions together with Snu17p and Pml1 as part of a nuclear pre-mRNA retention complex (Brooks et al. 2009). Single deletion of *BUD13* results in the accumulation of intron relative to exon signal, consistent with it having an important role as part of the U2 snRNP in splicing activity (Fig. 3B). In the double *cwc21-Δ bud13-Δ* mutant, there is a further increase in intron signal relative to exon signal as compared to either the *isy1-Δ* or *bud13-Δ* single mutants, indicating that Cwc21 and Bud13, like Cwc21 and Isy1, function together to support the formation of active splicing complexes. Notably, however, in contrast to the *cwc21-Δ isy1-Δ* double mutant, in the *cwc21-Δ bud13-Δ* double mutant it is apparent when comparing exon signals that there is a further decrease in transcript levels as compared to the levels observed in the *cwc21-Δ* mutant (Supplemental Fig. 1B). Given the role of Bud13 in retention of pre-mRNA in the nucleus (see Introduction), this finding suggests that the combined loss of Cwc21 and Bud13 could lead to a further increase in the levels of unspliced transcripts released from the nucleus, which are subsequently subject to turnover by NMD. It is interesting to note in this context that both Cwc21 and Bud13 are associated with U2 snRNP components including the retention and first step splicing factor Snu17 (Gottschalk et al. 2001; Trowitzsch et al. 2008; Brooks et al. 2009; this study), and their simultaneous loss from this snRNP particle could exacerbate disruptive effects on both pre-mRNA splicing and retention in the nucleus.

The effects on splicing in the single and double mutant strains observed by microarray analysis were confirmed using independent RT-PCR assays and sequencing of the resulting products. Several genes including *GFI15*, *RPL30*, and *RPL39* displaying intron accumulation in the double mutants were selected for analysis. In all cases analyzed, a pattern of intron accumulation was observed that is consistent with the results observed from the microarray analysis (see Fig. 3C for a representative example; data not shown).

Finally, we also asked whether there are differential effects on splicing activity in the single and double mutant strains that might affect functionally related subsets of genes, as has been observed for certain splicing factor mutants by others (Clark et al. 2002; Pleiss et al. 2007a,b). Using the tiling microarray data described above, genes were clustered based on differences in the relative ratios of intron-to-exon signals detected in the single and double mutants. We indeed detect transcripts from specific subsets of genes with apparent differences in intron levels (Fig. 3D; Supplemental Fig. 2). Gene Ontology (GO) enrichment analysis on the sets of genes within each distinct cluster shown in Figure 3D and Supplemental Figure 2 revealed significant enrichment for functional categories including "translation," "post-translational modification," and "reproduction." These categories were significantly enriched when the GO analysis was performed by comparing genes in the clusters against all profiled genes (Pg), or only intron-containing genes (Pi) (for cluster-specific *P*-values, see Fig. 3D and Supplemental Fig. 2).

Yeast Cwc21 and its human ortholog SRm300: Roles at the core of the spliceosome

In this study, we have investigated the function of the splicing-associated protein Cwc21 using a combination of genetic interaction analysis, mass spectrometry, and microarray profiling. The results provide evidence for an important and intimate function for Cwc21 in the formation of active step I spliceosomes. While our experiments do not reveal the precise biochemical role of Cwc21 in splicing (which may ultimately require a structure of core spliceosomal complexes to determine), they do reveal several spliceosomal proteins that likely function in close association with Cwc21. In particular, the genetic and physical association with Isy1 as well as with other factors that

participate in both splicing catalysis and fidelity, including U6 snRNA and Prp8 (Grainger and Beggs 2005; Grainger et al. 2009), suggests that Cwc21 could act to support a role in fidelity. This possibility is consistent with the observation that Cwc21 is not essential for yeast cell viability, that SRm300 is not obligatory for splicing catalysis (Blencowe et al. 2000), and that these proteins form part of the salt-resistant core of the step I spliceosomal complexes (Bessonov et al. 2008; P Fabrizio and R Lührmann, pers. comm.). However, our tiling microarray analysis and subsequent RT-PCR assays of transcripts in the single and double mutants did not reveal any aberrantly spliced products (data not shown), only differences in the efficiency of splicing.

Therefore, another possibility is that Cwc21 is one of several components, which are at least partially redundant, that configure the core of the spliceosome such that it is primed for splicing catalysis. It is interesting in this regard to consider the striking structural differences between Cwc21 and SRm300. While mammalian SRm300 shares significant similarity within its N-terminal domain with Cwc21, the mammalian protein contains a remarkably long C-terminal region that is highly enriched in alternating Arg/Ser dipeptide repeats (RS domains) and other repetitive features. SR family and SR-related proteins, which share the common feature of one or more RS domains, play numerous critical roles in the regulation of splice site selection (Lin and Fu 2007; Long and Caceres 2009). The RS domains of SR proteins are thought to interact with one another and with critical sites on pre-mRNA during the formation of splicing complexes (Lin and Fu 2007; Long and Caceres 2009). Indeed, SRm300 is the largest known SR-related protein (Blencowe et al. 2000). It is therefore interesting to consider that the RS domains and other repetitive regions of this protein not found in Cwc21 might provide a "buffer" between the flexibility required for regulated alternative splicing and a core activity required to support splicing catalysis. For example, SRm300 could function to "transmit" an appropriate conformation required for first step chemistry and this conformation could arise through diverse possible interaction pathways via the repetitive domains of SRm300 during spliceosome formation on constitutively and alternative spliced substrates. Consistent with this proposal, SRm300 forms a complex containing multiple factors involved in both constitutive and regulated splicing, including the splicing coactivator SRm160 and SR family proteins (Blencowe et al. 1998). Moreover, the observation that knockdown of the *C. elegans* ortholog of SRm300 disrupts early development suggests a possible critical, gene-specific role for this protein in splicing activity.

In regard to the above, it is interesting to note that in the present study, deletion of *CWC21*, alone and in combination with *ISY1* and *BUD13*, resulted in differential effects on splicing that affected specific subsets of functionally related genes, as has been observed for other splicing factor mutants (Pleiss et al. 2007a,b). Taken together, these results suggest that Cwc21 may also have gene-specific roles in splicing. Moreover, the genetic and physical interactions observed between Cwc21 and the SR-like factor Npl3, which functions in splicing, 3′-end formation, and export (Flach et al. 1994; Lee et al. 1996; Kress et al. 2008), suggest that, like SRm300, Cwc21 could function together with one or more SR-related proteins in yeast.

Finally, in addition to one or more direct roles in splicing, the systematic characterization of the genetic, physical, and functional interactions involving Cwc21 in this study has further suggested additional functional roles in aspects of mRNA biogenesis in *S. cerevisiae*, including snRNP formation and nuclear retention of pre-mRNA.

MATERIALS AND METHODS

Synthetic genetic arrays

Synthetic genetic array (SGA) analysis (Tong et al. 2004) was carried out in a high-density E-MAP format (Wilmes et al. 2008). Growth rates of the double mutants were assessed by automated image analysis of colony size, and a modified *t*-score (*S*) was calculated as previously described (Schuldiner et al. 2005; Collins et al. 2006).

Purification of TAP-tagged complexes

Tagged Prp8 and Cwc21 complexes were purified on immunoglobulin G (IgG) and calmodulin columns from yeast cell extracts (3–5 L) grown in yeast extract-peptone-dextrose (YEPD) medium to an OD_{600} of 1.0–1.5. Purification steps were performed essentially as previously described (Krogan et al. 2006). Eluted proteins were lyophilized or concentrated by precipitation with acetone or trichloroacetic acid (TCA). Purified proteins were separated by SDS-PAGE on gels containing 10% polyacrylamide, and the proteins were visualized by silver staining (data not shown).

For mass spectrometry analysis, TAP-tagged proteins were purified essentially as described previously (Krogan et al. 2006) except that sodium chloride was replaced with ammonium bicarbonate and Triton X-100 was omitted from the calmodulin washing buffer (10 mM Tris-Cl at pH 8, 100 mM ammonium bicarbonate, 10 mM β-mercaptoethanol, 0.1 mM $CaCl_2$) and the calmodulin elution buffer (10 mM Tris-Cl at pH 8, 100 mM ammonium bicarbonate, 10 mM β-mercaptoethanol, 3 mM EGTA at pH 8.0) to facilitate further analysis by LC-MS. Peptides for all proteins listed in Table 1 were detected by LC-MS at a confidence of 99.6%. Confidence levels were assigned to the mass spectra using STATQUEST, as described previously (Kislinger et al. 2003). Analysis of the mass spectrometry data sets to identify proteins that are specifically associated with the tagged proteins was performed as described previously (Collins et al. 2007).

Profiling of noncoding RNA associated with TAP-tagged complexes

RNA was isolated from the TAP Cwc21p and Prp8p complexes and whole-cell extracts by phenol/chloroform extraction followed by incubation with DNase I for 30 min at 37°C (5 mL DNase I/10 μg of

RNA). A second phenol/chloroform extraction was performed, followed by ethanol precipitation. RNA samples were suspended in 1× labeling buffer (TE: 5 mM Tris, 1 mM EDTA at pH 7.8) and directly labeled with Cy3 and Cy5 dyes as previously described (Hiley et al. 2005). Labeled RNAs were hybridized for 16–20 h at 42°C to a custom Agilent microarray containing tiling probes (spaced by 20 nucleotides) specific for *S. cerevisiae* non-coding RNAs (Hiley et al. 2005). Slides were scanned using an Agilent model G2565BA scanner. Spot quantification was carried out using Imagene 7.5 (Biodiscovery), and the microarray data were lowess-normalized using the Marray package from Bioconductor (Gentleman et al. 2004).

Tiling array analyses of single and double deletion mutants

A wild-type (WT) strain and single and double deletion strains for *CWC21*, *ISY1*, and/or *BUD13* were grown in YPD medium at 30°C until mid-log phase (OD_{600} = 0.8). The single mutants were made by directly transforming an "α" strain (Y3656 or a similar strain) with the NatR cassette flanked by gene-specific primers (Schuldiner et al. 2005). To obtain double mutants, the "α" strain mutants (NatR) were crossed with "**a**" strain mutants (KanR). Diploids were selected and then sporulated and dissected. The tetrads were then genotyped by replica-plating on Kan(G418) and/or Nat medium. Isolation of total RNA from the samples and hybridization to the yeast tiling array were performed according to Juneau et al. (2007), except that Actinomycin D was added to a final concentration of 6 μg/mL during cDNA synthesis to prevent antisense artifacts (Perocchi et al. 2007). Tiling arrays were quantile normalized in pairs with the Affymetrix Tiling Analysis Software (TAS) v1.1 using perfect-match probes only and a bandwidth of 20, setting the mutant strains as the "treatment" and the WT strain as the "control" channel. Average changes in expression across introns and exons of intron-containing genes in the mutant versus WT strains were calculated across all probes fully contained within these regions. The change in intron expression was then corrected for expression changes in exons by taking the ratio of the two averages (Supplemental Table 1).

RT-PCR assays

Semi-quantitative RT-PCR assays were performed using the One-Step kit (QIAGEN) as recommended by the manufacturer. Thirty nanograms of yeast total RNA was used in each reaction. Amplified cDNA products corresponding to spliced and unspliced transcripts were resolved on a 2% agarose gel and stained with ethidium bromide. Relative intensities of products were quantified using ImageJ software. The sequences of the primers (directed to exon sequences) used in reactions are available upon request.

Microarray data

Microarray data are available from the GEO database (accession number GSE17395).

SUPPLEMENTAL MATERIAL

Supplemental material can be found at http://www.rnajournal.org.

ACKNOWLEDGMENTS

We thank Corey Nislow for generously sharing reagents and equipment used in the tiling microarray analysis, Brenda Andrews and Charlie Boone for providing strains, and Deb Ray for helpful comments on the manuscript. We also thank Jean Beggs, Patricia Fabrizio, and Reinhard Lührmann for helpful discussions and kindly communicating results prior to publication. This research was supported by a grant from the Canadian Institutes of Health Research (MOP-14609) to B.J.B. H.V.B. was supported by fellowships from The Netherlands Organisation for Scientific Research and from the CIHR.

Received June 20, 2009; accepted August 18, 2009.

REFERENCES

Abovich N, Liao XC, Rosbash M. 1994. The yeast MUD2 protein: An interaction with PRP11 defines a bridge between commitment complexes and U2 snRNP addition. *Genes & Dev* **8:** 843–854.

Bessonov S, Anokhina M, Will CL, Urlaub H, Lührmann R. 2008. Isolation of an active step I spliceosome and composition of its RNP core. *Nature* **452:** 846–850.

Blencowe BJ, Issner R, Nickerson JA, Sharp PA. 1998. A coactivator of pre-mRNA splicing. *Genes & Dev* **12:** 996–1009.

Blencowe BJ, Bauren G, Eldridge AG, Issner R, Nickerson JA, Rosonina E, Sharp PA. 2000. The SRm160/300 splicing coactivator subunits. *RNA* **6:** 111–120.

Brooks MA, Dziembowski A, Quevillon-Cheruel S, Henriot V, Faux C, van Tilbeurgh H, Seraphin B. 2009. Structure of the yeast Pml1 splicing factor and its integration into the RES complex. *Nucleic Acids Res* **37:** 129–143.

Caspary F, Seraphin B. 1998. The yeast U2A′/U2B complex is required for pre-spliceosome formation. *EMBO J* **17:** 6348–6358.

Chan SP, Cheng SC. 2005. The Prp19-associated complex is required for specifying interactions of U5 and U6 with pre-mRNA during spliceosome activation. *J Biol Chem* **280:** 31190–31199.

Chan SP, Kao DI, Tsai WY, Cheng SC. 2003. The Prp19p-associated complex in spliceosome activation. *Science* **302:** 279–282.

Chen HR, Jan SP, Tsao TY, Sheu YJ, Banroques J, Cheng SC. 1998. Snt309p, a component of the Prp19p-associated complex that interacts with Prp19p and associates with the spliceosome simultaneously with or immediately after dissociation of U4 in the same manner as Prp19p. *Mol Cell Biol* **18:** 2196–2204.

Clark TA, Sugnet CW, Ares M Jr. 2002. Genomewide analysis of mRNA processing in yeast using splicing-specific microarrays. *Science* **296:** 907–910.

Collins SR, Schuldiner M, Krogan NJ, Weissman JS. 2006. A strategy for extracting and analyzing large-scale quantitative epistatic interaction data. *Genome Biol* **7:** R63. doi: 10.1186/gb-2006-7-7-r63.

Collins SR, Kemmeren P, Zhao XC, Greenblatt JF, Spencer F, Holstege FC, Weissman JS, Krogan NJ. 2007. Toward a comprehensive atlas of the physical interactome of *Saccharomyces cerevisiae*. *Mol Cell Proteomics* **6:** 439–450.

Das B, Das S, Sherman F. 2006. Mutant LYS2 mRNAs retained and degraded in the nucleus of *Saccharomyces cerevisiae*. *Proc Natl Acad Sci* **103:** 10871–10876.

Dix I, Russell C, Yehuda SB, Kupiec M, Beggs JD. 1999. The identification and characterization of a novel splicing protein, Isy1p, of *Saccharomyces cerevisiae*. *RNA* **5:** 360–368.

Dziembowski A, Ventura AP, Rutz B, Caspary F, Faux C, Halgand F, Laprevote O, Seraphin B. 2004. Proteomic analysis identifies a new complex required for nuclear pre-mRNA retention and splicing. *EMBO J* **23:** 4847–4856.

Fernandez CF, Pannone BK, Chen X, Fuchs G, Wolin SL. 2004. An Lsm2–Lsm7 complex in *Saccharomyces cerevisiae* associates with the small nucleolar RNA snR5. *Mol Biol Cell* **15:** 2842–2852.

Flach J, Bossie M, Vogel J, Corbett A, Jinks T, Willins DA, Silver PA. 1994. A yeast RNA-binding protein shuttles between the nucleus and the cytoplasm. *Mol Cell Biol* **14:** 8399–8407.

Gavin AC, Aloy P, Grandi P, Krause R, Boesche M, Marzioch M, Rau C, Jensen LJ, Bastuck S, Dumpelfeld B, et al. 2006. Proteome survey reveals modularity of the yeast cell machinery. *Nature* **440:** 631–636.

Gentleman RC, Carey VJ, Bates DM, Bolstad B, Dettling M, Dudoit S, Ellis B, Gautier L, Ge Y, Gentry J, et al. 2004. Bioconductor: Open software development for computational biology and bioinformatics. *Genome Biol* **5:** R80. doi: 10.1186/gb-2004-5-10-r80.

Gottschalk A, Bartels C, Neubauer G, Lührmann R, Fabrizio P. 2001. A novel yeast U2 snRNP protein, Snu17p, is required for the first catalytic step of splicing and for progression of spliceosome assembly. *Mol Cell Biol* **21:** 3037–3046.

Grainger RJ, Beggs JD. 2005. Prp8 protein: At the heart of the spliceosome. *RNA* **11:** 533–557.

Grainger RJ, Barrass JD, Jacquier A, Rain J-C, Beggs JD. 2009. Physical and genetic interactions of yeast Cwc21p, an ortholog of human SRm300/SRRM2, suggest a role at the catalytic center of the spliceosome. *RNA* (this issue). doi: 10.1261/rna.1908309.

He F, Peltz SW, Donahue JL, Rosbash M, Jacobson A. 1993. Stabilization and ribosome association of unspliced pre-mRNAs in a yeast upf1-mutant. *Proc Natl Acad Sci* **90:** 7034–7038.

Hiley SL, Babak T, Hughes TR. 2005. Global analysis of yeast RNA processing identifies new targets of RNase III and uncovers a link between tRNA 5′ end processing and tRNA splicing. *Nucleic Acids Res* **33:** 3048–3056.

Juneau K, Palm C, Miranda M, Davis RW. 2007. High-density yeast-tiling array reveals previously undiscovered introns and extensive regulation of meiotic splicing. *Proc Natl Acad Sci* **104:** 1522–1527.

Kislinger T, Rahman K, Radulovic D, Cox B, Rossant J, Emili A. 2003. PRISM, a generic large scale proteomic investigation strategy for mammals. *Mol Cell Proteomics* **2:** 96–106.

Kress TL, Krogan NJ, Guthrie C. 2008. A single SR-like protein, Npl3, promotes pre-mRNA splicing in budding yeast. *Mol Cell* **32:** 727–734.

Krogan NJ, Cagney G, Yu H, Zhong G, Guo X, Ignatchenko A, Li J, Pu S, Datta N, Tikuisis AP, et al. 2006. Global landscape of protein complexes in the yeast *Saccharomyces cerevisiae*. *Nature* **440:** 637–643.

Lee MS, Henry M, Silver PA. 1996. A protein that shuttles between the nucleus and the cytoplasm is an important mediator of RNA export. *Genes & Dev* **10:** 1233–1246.

Leeds NB, Small EC, Hiley SL, Hughes TR, Staley JP. 2006. The splicing factor Prp43p, a DEAH box ATPase, functions in ribosome biogenesis. *Mol Cell Biol* **26:** 513–522.

Lin S, Fu XD. 2007. SR proteins and related factors in alternative splicing. *Adv Exp Med Biol* **623:** 107–122.

Long JC, Caceres JF. 2009. The SR protein family of splicing factors: Master regulators of gene expression. *Biochem J* **417:** 15–27.

Longman D, McGarvey T, McCracken S, Johnstone IL, Blencowe BJ, Caceres JF. 2001. Multiple interactions between SRm160 and SR family proteins in enhancer-dependent splicing and development of *C. elegans*. *Curr Biol* **11:** 1923–1933.

Matlin AJ, Moore MJ. 2007. Spliceosome assembly and composition. *Adv Exp Med Biol* **623:** 14–35.

Noble SM, Guthrie C. 1996a. Identification of novel genes required for yeast pre-mRNA splicing by means of cold-sensitive mutations. *Genetics* **143:** 67–80.

Noble SM, Guthrie C. 1996b. Transcriptional pulse-chase analysis reveals a role for a novel snRNP-associated protein in the manufacture of spliceosomal snRNPs. *EMBO J* **15:** 4368–4379.

Ohi MD, Gould KL. 2002. Characterization of interactions among the Cef1p-Prp19p-associated splicing complex. *RNA* **8:** 798–815.

Ohi MD, Link AJ, Ren L, Jennings JL, McDonald WH, Gould KL. 2002. Proteomics analysis reveals stable multiprotein complexes in both fission and budding yeasts containing Myb-related Cdc5p/Cef1p, novel pre-mRNA splicing factors, and snRNAs. *Mol Cell Biol* **22:** 2011–2024.

Pannone BK, Kim SD, Noe DA, Wolin SL. 2001. Multiple functional interactions between components of the Lsm2–Lsm8 complex, U6 snRNA, and the yeast La protein. *Genetics* **158:** 187–196.

Perocchi F, Xu Z, Clauder-Munster S, Steinmetz LM. 2007. Antisense artifacts in transcriptome microarray experiments are resolved by actinomycin D. *Nucleic Acids Res* **35:** e128. doi: 10.1093/nar/gkm683.

Pleiss JA, Whitworth GB, Bergkessel M, Guthrie C. 2007a. Rapid, transcript-specific changes in splicing in response to environmental stress. *Mol Cell* **27:** 928–937.

Pleiss JA, Whitworth GB, Bergkessel M, Guthrie C. 2007b. Transcript specificity in yeast pre-mRNA splicing revealed by mutations in core spliceosomal components. *PLoS Biol* **5:** e90. doi: 10.1371/journal.pbio.0050090.

Puig O, Caspary F, Rigaut G, Rutz B, Bouveret E, Bragado-Nilsson E, Wilm M, Seraphin B. 2001. The tandem affinity purification (TAP) method: A general procedure of protein complex purification. *Methods* **24:** 218–229.

Rutz B, Seraphin B. 1999. Transient interaction of BBP/ScSF1 and Mud2 with the splicing machinery affects the kinetics of spliceosome assembly. *RNA* **5:** 819–831.

Sayani S, Janis M, Lee CY, Toesca I, Chanfreau GF. 2008. Widespread impact of nonsense-mediated mRNA decay on the yeast intronome. *Mol Cell* **31:** 360–370.

Schuldiner M, Collins SR, Thompson NJ, Denic V, Bhamidipati A, Punna T, Ihmels J, Andrews B, Boone C, Greenblatt JF, et al. 2005. Exploration of the function and organization of the yeast early secretory pathway through an epistatic miniarray profile. *Cell* **123:** 507–519.

Staley JP, Woolford JL Jr. 2009. Assembly of ribosomes and spliceosomes: Complex ribonucleoprotein machines. *Curr Opin Cell Biol* **21:** 109–118.

Stevens SW, Barta I, Ge HY, Moore RE, Young MK, Lee TD, Abelson J. 2001. Biochemical and genetic analyses of the U5, U6, and U4/U6•U5 small nuclear ribonucleoproteins from *Saccharomyces cerevisiae*. *RNA* **7:** 1543–1553.

Szymczyna BR, Bowman J, McCracken S, Pineda-Lucena A, Lu Y, Cox B, Lambermon M, Graveley BR, Arrowsmith CH, Blencowe BJ. 2003. Structure and function of the PWI motif: A novel nucleic acid-binding domain that facilitates pre-mRNA processing. *Genes & Dev* **17:** 461–475.

Tharun S, He W, Mayes AE, Lennertz P, Beggs JD, Parker R. 2000. Yeast Sm-like proteins function in mRNA decapping and decay. *Nature* **404:** 515–518.

Tong AH, Evangelista M, Parsons AB, Xu H, Bader GD, Page N, Robinson M, Raghibizadeh S, Hogue CW, Bussey H, et al. 2001. Systematic genetic analysis with ordered arrays of yeast deletion mutants. *Science* **294:** 2364–2368.

Tong AH, Lesage G, Bader GD, Ding H, Xu H, Xin X, Young J, Berriz GF, Brost RL, Chang M, et al. 2004. Global mapping of the yeast genetic interaction network. *Science* **303:** 808–813.

Trowitzsch S, Weber G, Lührmann R, Wahl MC. 2008. An unusual RNA recognition motif acts as a scaffold for multiple proteins in the pre-mRNA retention and splicing complex. *J Biol Chem* **283:** 32317–32327.

Villa T, Guthrie C. 2005. The Isy1p component of the NineTeen Complex interacts with the ATPase Prp16p to regulate the fidelity of pre-mRNA splicing. *Genes & Dev* **19:** 1894–1904.

Vincent K, Wang Q, Jay S, Hobbs K, Rymond BC. 2003. Genetic interactions with CLF1 identify additional pre-mRNA splicing factors and a link between activators of yeast vesicular transport and splicing. *Genetics* **164:** 895–907.

Volckaert G, Voet M, Van der Schueren J, Robben J, Vanstreels E, Vander Stappen J. 2003. Disruption of 12 ORFs located on chromosomes IV, VII and XIV of *Saccharomyces cerevisiae* reveals two essential genes. *Yeast* **20:** 79–88.

Wahl MC, Will CL, Lührmann R. 2009. The spliceosome: Design principles of a dynamic RNP machine. *Cell* **136:** 701–718.

Wilmes GM, Bergkessel M, Bandyopadhyay S, Shales M, Braberg H, Cagney G, Collins SR, Whitworth GB, Kress TL, Weissman JS, et al. 2008. A genetic interaction map of RNA-processing factors reveals links between Sem1/Dss1-containing complexes and mRNA export and splicing. *Mol Cell* **32:** 735–746.

Xu D, Friesen JD. 2001. Splicing factor slt11p and its involvement in formation of U2/U6 helix II in activation of the yeast spliceosome. *Mol Cell Biol* **21:** 1011–1023.

Zhao R, Kakihara Y, Gribun A, Huen J, Yang G, Khanna M, Costanzo M, Brost RL, Boone C, Hughes TR, et al. 2008. Molecular chaperone Hsp90 stabilizes Pih1/Nop17 to maintain R2TP complex activity that regulates snoRNA accumulation. *J Cell Biol* **180:** 563–578.